Detecting and Tracking Multi-Object in Real Marine Environment

M. Martelli[a*], N. Faggioni[a], F. Ponzini[a]

[a]*Dept. of Marine, Electrical, Electronic, Telecommunications Engineering and Naval Architecture (DITEN), Polytechnic School of Genoa University, Genova, Italy*

*Corresponding author. Email: michele.martelli@unige.it

Synopsis

In recent years, the maritime sector has been witnessing a growing interest in autonomous navigation due to its advantages in safety. Within this framework, it is challenging to have available an automatic collision avoidance system based on data coming from the onboard sensors. For instance, LiDAR (Light Detection and Ranging) sensors are often employed to obtain a virtualized model of the surrounding environment in order to obtain an increase of situational awareness. Deep Learning approaches are widely used in the automotive sector for obstacle detection, particularly, trained Convolutional Neural Networks. Still, they imply a training phase based on a large dataset of pre-labelled LiDAR scans. Unfortunately, an extensive training dataset is not yet available for the marine environment. For such a reason, this paper presents in detail a low-computational alternative procedure based on Unsupervised Learning which overcomes the lack of a training dataset; each step is investigated, from the data sampling up to the multi-target tracking of the detected obstacles. In particular, the proposed object detection framework has been tested by means of an extensive on-field data collection campaign carried out during sea trials by equipping a ship with a LiDAR. Furthermore, Euclidean distance-based clustering algorithm and a bounding-box construction method based on Principal Component Analysis have been adopted. Moreover, a specific tracking system with no prediction filters is proposed to fulfil the strict time constraint for fast reactions in complex scenarios where several objects need to be tracked. The algorithm has been tested versus the well-known Global Nearest Neighbour tracker; such a comparison includes the computational cost and the results' accuracy. The whole approach has been tested on such a challenging and dynamic marine scenario, and the results obtained are presented and discussed. Such and outcome shows that the proposed approach can detect and track multiple objects with reasonable accuracy; moreover, the outputs are provided near real-time. To conclude, the pros, the weaknesses, and future developments are reported.

Keywords: LiDAR Point Cloud, Multi-Object Tracking, Sea Trials, Autonomous Ship, Collision Detection, Unsupervised Learning.

1 Introduction

The autonomous vehicles research field has been gaining a big interest in recent years, involving several applications and consequent investments; the marine sector, and in particular the ASVs (Autonomous Surface Vehicles) segment, is not excluded (Schiaretti et al., 2017a).

The surface units navigate in an operating environment which is populated by non-cooperative agents, fixed or dynamic, which can pose a serious risk of collision, with implications for safety, environmental pollution, and economic damages.

Marine units can benefit from the increased level of autonomy implemented on board to mitigate the risks associated with navigation in crowded areas.

Technologies suitable to achieve autonomous navigation have been studied for the last decade and they still represent challenging topics.

With the aim of increasing the level of autonomy implemented on board (Schiaretti et al., 2017b), the Guidance, Navigation, and Control (GNC) systems are profoundly analysed by both civil and military companies, and research institutes as well; specifically, Obstacle Detection and Tracking systems play a key role within the navigation module, improving the ASV's perception of the surrounding environment. Moreover, the development of

Authors' Biographies

Prof. Michele Martelli received his B.Sc., M.Sc. and PhD degrees in Naval Architecture and Marine Engineering from Genoa University (Italy) in 2006, 2009 and 2013. From 2014 to 2016, as a post-doc, he worked on two research projects dealing with the autonomous capabilities of ships and small crafts. He joined as Assistant Professor at the DITEN Department, University of Genoa, in 2016. In 2019 he has been appointed as Associate Professor in the same Department. Since the beginning of his PhD, he has been involved in several national and international projects either as a researcher or as the principal investigator; he published over 60 peer-reviewed articles. He is a reviewer for several high-ranked journals and part of several international scientific committees.

Dr. Nicolò Faggioni was born in Italy in 1991. He received his Bachelor's degree in Nautical Engineering in 2014, a Master's degree in Yacht Design in 2017 and a PhD degree in autonomous navigation topic in 2022 from the University of Genoa. Currently, he is working for Fincantieri NexTech company on automation and control systems for the marine sector. His main research interests concern ship propulsion plants, mathematical models and numerical simulation.

Eng. Filippo Ponzini was born in Italy in 1996. He received his B.Sc. and M.Sc. in Naval Architecture and Marine Engineering from Genoa University (Italy) in 2019, 2021. Currently he is collaborating with the Genoa University in autonomous navigation research activity at the DITEN Department. His main research interests concern autonomous and unmanned surface vehicles development, marine robotics and ship propulsion plants.

 https://doi.org/10.24868/10707

such a system represents a significant prerequisite for an effective Collision Avoidance logic.
AIS (Automatic Identification System) can constitute a useful ally to face these issues - a numeric geometrical approach for collision avoidance is discussed in (Zaccone and Martelli, 2020) - but it does not cover all units (only cargo ships of 300 gross tonnages or more and all passenger ships are equipped with AIS).
Small leisure yachts and small ASVs/USVs are typically AIS unequipped, despite they operate in conditions with a relevant risk of collision. Thus, this paper presents a low computational solution, customized for the marine environment, to achieve Obstacle Detection (OD) and Multi-Target Tracking (MTT) for AIS unequipped vessels analysing Light Detection and Ranging (LiDAR) devices output. In particular, the procedure is tailored for medium-small size vessels that need a fast and effective obstacles detection at close distances (<100m), such as for the cases of un/berthing, harbour navigation and coastal patrol; indeed, the waters immediately surrounding the ASV can be populated by non-cooperative agents such as swimmers, small fishing boats, buoys, wreckages and other obstacles, often not detectable with any sensors (Clunie et al., 2021).
Vessel detection at short-range using RADARs is challenging due to their inherent shadow zone (Han et al., 2017); in such a scenario, LiDAR-based obstacle detection and tracking procedure could play a key role in filling the leaks of other sensors such as cameras and RADARs in a multi-sensor collision avoidance system. Infact, the use of a heterogeneous number of sensors with different peculiarities and measurement ranges allows the effectiveness of the system to be extended to broader scenarios, covering and balancing the shortcomings of individual sensors. A method for dealing with obstacle detection in LiDAR and cameras is proposed in (Faggioni et al., 2022).Figure 1 shows a possible application of the discussed procedure in a multi-sensor data fusion perceptive system. In paritcular, obstacles are detected in the LiDAR point cloud and the acquired targets are tracked by adopting a low computational customized method, instead of the probabilistic approaches generally employed (Ruud et al., 2018) (Lee et al., 2010). To simplify the handling of the problem, tracking is performed on the centroids of the point clouds; such an approach is often adopted to decrease the computational cost (Fang et al., 2016). Under this idea, the procedure ensures a low computational effort to guarantee a reaction time compatible with avoidance manoeuvres, especially in ASV-obstacle short-range conditions, exploiting the peculiarities that a LiDAR device ensures over short distances.
Long-range LiDARs are however available in the market, the proposed procedure is scalable for devices that provide an output in the same form.

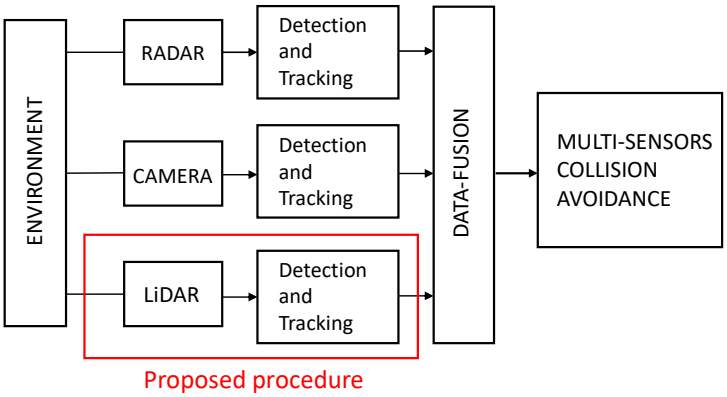

Figure 1: Multi-sensor collision avoidance system.

2 Methodology

The proposed method of obstacle detection and tracking is performed through several steps or modules (see Figure 2). First, the data regarding the surrounding environment is acquired by the LiDAR sensor to obtain a computer representation of the physical scenario. In the second procedure step, obstacles that populate the scan are detected by means of unsupervised machine learning methods. Eventually, obstacles detected are tracked in the time domain. The idea is to detect obstacles that populate the LiDAR point cloud and to keep track of their position and motions by processing the representative centroid with a tracking engine. Carrying out the obstacle detection activity in a point-cloud virtualised environment means to group points that constitute items and to assign to each group size and position. The use of supervised approaches for obstacle detection, such as Convolutional Neural Network (CNN), is widely documented in the literature with appreciable results (Iqbal et al., 2021). Despite this, the authors present a method based on unsupervised machine learning that allows overcoming the training activity

 https://doi.org/10.24868/10707

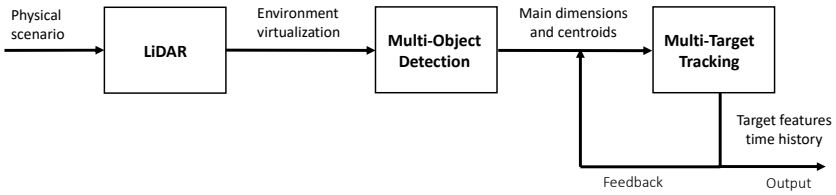

Figure 2: Proposed system workflow.

that a supervised approach needs; this is necessary since no marine training pre-labelled dataset is yet available for direct use as it is for the automotive sector (Geiger et al., 2013), where the available financial resources and the mass production are more significant.
Under the idea of breaking down the computational cost, which is a priority in real-time conditions, the tracking activity is performed on centroids only and the track assignment is simplified in a minimum-distance-based logic excluding prediction filters.

3 Multi-Obstacle Detection

In this section, the unsupervised machine learning procedures adopted to perform the obstacle detection activity on the LiDAR point cloud are deepened. Figure 3 gives the workflow of the obstacle detection module. Specifically, the raw output of the LiDAR sensor is first processed with an ad hoc filter. Points that constitute an obstacle are then grouped by employing a Euclidean distance-based Clustering algorithm. Finally, to each group it is assigned a bounding box created by means of Principal Component Analysis and a representative centroid. Such a procedure allows to detect obstacles and assign them approximated dimensions and positions. In order to decrease the computational effort, the analysis is performed working on an x-y bidimensional plane where z is the vertical component; however, the information regarding the third dimension is still available in any working step.

3.1 Noise Filtering and Euclidean Clustering

Several noisy phenomena are captured within a LiDAR acquisition in the marine environment, such as wake reflection and acquisition errors. The points that can be classified as noise are typically found at sea level and have a low level of intensity; the addition of noise filters allows cleaning the scenario from any interference. In order to preserve the hull points, the filter excludes only points with a vertical position lower than a threshold value, identified by the sea level and, simultaneously, with a value of intensity lower than the typical value of the noisy points, which must be contextualized on the instrument used; for the case study, the intensity parameter can take values ranging from 0 to 256.
Clustering a point cloud is a widely documented activity (Fritsch et al., 2013) (Song et al., 2019) and means to group points belonging to the same objects that share a certain similarity. Such activity is achieved by various algorithms that differ significantly in the definition of what constitutes a cluster. For the case study, a Euclidean distance-based clustering algorithm is selected; this algorithm allows to obtain reasonably accurate results in extremely low computational effort, thanks to its simplicity if compared to the others. The procedure is indeed based

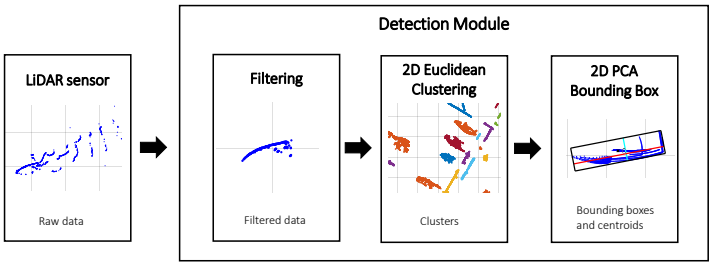

Figure 3: Main step of the detection module.

 https://doi.org/10.24868/10707

on a single threshold parameter, the Euclidean distance; points are segmented within the same group if their reciprocal distance is less than or equal to the threshold distance ε. In addition, the minimum number of points required to form a cluster (*minNCP*) was set; this further eliminates noisy points that eluded the action of the intensity filter. The combined action of clustering and filtering analysis allows obtaining the groups of points that represent the obstacles in a scenario free from any interference.
Given the raw point cloud, the required actions to identify a cluster are schematically outlined below:

1. Points with an intensity value equal to or below the set parameter (intesity limit) and simultaneously located at or below sea level are eliminated.
2. Points placed at an Euclidean distance equal to or less than the ε parameter are grouped in the same cluster.
3. Clusters populated by fewer points than the *minNCP* parameter are eliminated.

3.2 Bounding-Boxing and Principal Component Analysis

In order to obtain a single representative point and the main dimensions of obstacles detected, the clustering analysis output must be processed; in this paper, such analysis is done via the bounding-box approach.
The chosen method to build a bounding box on a group of points, among the many presented in the literature, is the PCA (Principal Components Analysis) approach (Jolliffe, 2002) (Jackson, 1988). It guarantees a convenient balance between the quality of the representation and the computational load. In particular, Principal Component Analysis allows the possibility of obtaining a bounding box oriented according to the greatest variance dimensions of the distribution of points.
The definition of centroid adopted to obtain a representative point of the distribution of points is the geometric centre of the bounding box. From a statistical point of view, the centroid would be defined as the centre of the distribution of the points, which is easily calculated in a LiDAR scan. Contextualizing the problem from an operational and experimental point of view, the centre of the bounding box however guarantees a more faithful representation of the real centre of the obstacle. The peculiarities of a LiDAR scan imply indeed a greater density of the object representative points towards the first impact surfaces of the laser channels; the use of the geometric centre of the bounding box can partially compensate for this phenomenon.
Given a cluster, the required actions to a bounding box and the centroid are schematically outlined below:

1. Principal Component Analysis is performed on the cluster point cloud. The two perpendicular directions of maximum variance are computed. Moreover, the mean and the projection of the points on the two directions obtained are calculated.
2. The point projections on the two directions of maximum variance are employed to assess the limits of the bounding box.
3. The centroid is calculated as the geometric centre of the bounding box.

4 Multi-Target Tracking

Performing the tracking activity means following the detected targets along with the time domain. A track or identifier is assigned to the targets in order to collect the temporal evolution of position and other features of interest.
In the case study, tracking is performed only on the centroids of the bounding boxes, considered as a representative point of the vessel; knowing the time history of the positions occupied by the centroids also makes it possible to calculate the velocity and acceleration. Even though only centroids are tracked, the extent of the bounding box and the point cloud on which it was built remains linked to each point tracked at each time step. This allows for tracking both the kinematic characteristics and the spatial extent of the targets in the time domain. The objective is to obtain a fast method, tailored to the marine environment, that ensures multi-obstacle detection and tracking under real-time working assumptions. The speed of the algorithm is indeed crucial for integration with collision avoidance logic and automatic decision support systems in high-speed or low-distance scenarios. In the following chapters, the proposed low-computational method will be discussed and compared with the well-known Global Nearest Neighbour tracking system (Blackman, 1999), highlighting the pros and cons.

4.1 Proposed track-association algorithm

The main challenge that a multi-target-tracking algorithm must solve is the track-to-object assignment. If the acquired target is unique, the problem does not arise. However, with many sensors, representative target points obtained at successive acquisitions have a random identifier, if any. Therefore, the acquired object must be assigned

 https://doi.org/10.24868/10707

to a track (or have an identifier assigned to it) so that a time history can be constructed. The same problem occurs with LiDAR scans. In fact, although the clustering algorithm assigns a label to the identified clusters, it starts analysing the objects at a random seed point. The labels assigned to the clusters, therefore, have no consistency in the time domain. Furthermore, there is no assurance that the number of objects detected at time *t* and time *t-1* is the same. The proposed method for accomplishing the tracking task is based on proximity position logic. An object belonging to a generic time *t* is assigned the label that identifies the object of the previous time for which the distance is minimized. The distances between the clusters belonging to the present and immediate past scan are computed at each time step and stored in a matrix used for comparison. Additional tracks are initialised if the new scan is populated with more elements than the previous one and the unassigned objects are assigned to it. Instead, any unassigned track is closed. Despite its extreme simplicity, this procedure provides surprisingly accurate results when contextualised to the case study. The computational load is greatly reduced as track assignment is performed without the use of time-consuming predictive filters.
Given the set of centroids, the required actions for the track identifier assignment are schematically outlined below:

1. The mutual distances between the centroids of the current scan and the previous scan are calculated and stored in a Distance Matrix.
2. Let n be the number of targets in the current scan and m the number of targets in the previous scan.
    - If $n \leq m$, targets of the current scan are sequentially assigned to the track of the nearest target of the previous scan. Any unassigned tracks are deleted.
    - If $n > m$, targets of the current scan are sequentially assigned to the track of the nearest target of the previous scan until m allocations are reached. The remaining unassigned targets are assigned to a new track.
3. Given the time sequence of the positions of the centroids of each track, the velocity is calculated as the differential.

4.2 Global Nearest Neighbor

Global Nearest Neighbour (Konstantinova et al., 2003), abbreviated GNN, is a simple association algorithm for multi-target tracking systems capable of processing detections of many targets from multiple sensors. In a cluttered environment, the detections obtained may not all be attributable to real objects; the GNN algorithm tries to provide an optimal solution in a dense target environment, propagating the most likely hypothesis. The optimal assignment minimizes an overall distance function where the distance value is computed as a statistical distance function that considers all target-track assignments. In such an environment, gating activity around the predicted observation is necessary for eliminating unlikely observations. In particular, a Kalman filter is assumed to predict the observation position from the previous step to the current step.
GNN is known as a fast algorithm suitable for real-time implementation. GNN guarantees encouraging results in high-density scenarios, with false alarms and high detection rates. However, the results obtained show that the proposed association method guarantees much less computational time, producing the same results in the case study. A more in-depth discussion will be shown in the following chapters.

5 On-field Experimental Campaign

An extensive experimental campaign was carried out in order to collect a suitable marine dataset. In particular, the LiDAR device was mounted onboard a vessel about 18 m long, and used for research purposes. The test has been done in a crowded navigation area (Augusta (IT), bay and harbour) in December 2021, allowing capturing different operative scenarios. Specifically, the acquisition is entrusted to a HESAI Pandar XT LiDAR device, shown in Figure 4. In particular, Pandar XT is 3D rotating LiDAR which uses 32 equally spaced infrared laser beams and stores the output data in a point-cloud structure; for each acquired point are thus available a set of spatial coordinates in the sensor reference frame and an intensity value, depending on colour, shape, and laser encounter angle; a raw scan of a chemical tanker at anchor obtained using the discussed device is shown in Figure 5, and used as one of the two showcases presented in this paper.

Figure 6 shows different step of the experimental campaign. Specifically, from left to right are shown the LiDAR mounting operation, the LiDAR mounting layout, the chemical tanker scenario and, finally, the GPS track of the path followed during the sea trials.

In the paper are presented two half-minute acquisitions for tracking purposes. The first scenario shows the authors' vessel passing astern of a ship at anchor on the left. Meanwhile, a small pilot boat intercepts the vessel's course from port to starboard. The second scenario shows part of a series of turning manoeuvres performed near a chemical tanker at anchor.

 https://doi.org/10.24868/10707

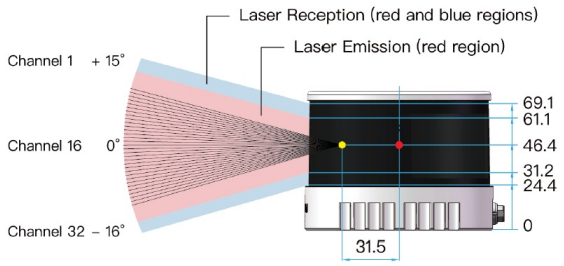

Figure 4: Hesai PandarXT

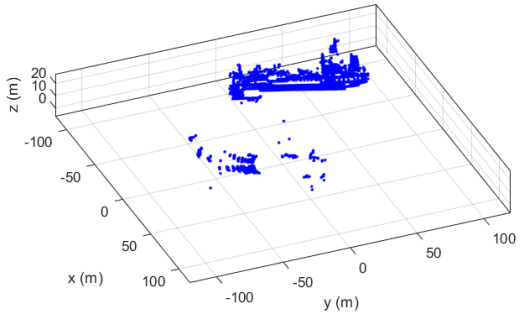

Figure 5: PandarXT scan of a chemical carrier.

Figure 6: On-field experimental campaign highlights.

The proposed series of scans permits an appreciation of the kinematics of the acquired targets in the ship's reference frame. However, the sensor's base (O_l, $\underline{l_1}$, $\underline{l_2}$, $\underline{l_3}$) does not coincide with the ship's one (O_b, $\underline{b_1}$, $\underline{b_2}$, $\underline{b_3}$), neither for the axis orientation nor for the position of the origin, as shown in Figure 7.

In order to express the acquired point clouds in the ship reference frame, it is therefore necessary to perform a base rotation. The following matrix $R_{l,b}$ is used to switch from sensor's base (O_l, $\underline{l_1}$, $\underline{l_2}$, $\underline{l_3}$) to ship's base (O_b, $\underline{b_1}$, $\underline{b_2}$, $\underline{b_3}$); in particular, Euler Angles θ and ψ are respectively identified around $\underline{l_2}$ and $\underline{l_3}$:

$$R_{l,b} = \begin{bmatrix} \cos\theta\cos\psi & \sin\psi & -\sin\theta\cos\psi \\ -\cos\theta\sin\psi & \cos\psi & \sin\theta\sin\psi \\ -\sin\theta & 0 & \cos\theta \end{bmatrix}$$

In particular, for the case study $\theta = 180°$ and $\psi = 90°$. Thus:

$$x_{1(b)} = x_{2(l)}$$

$$x_{2(b)} = x_{1(l)}$$

$$x_{3(b)} = -x_{3(l)}$$

 https://doi.org/10.24868/10707

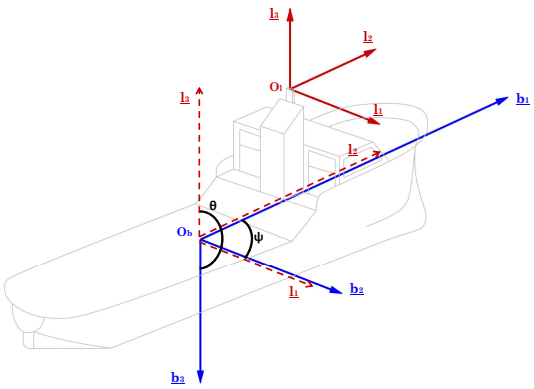

Figure 7: Lidar's and ship's reference frames.

6 Results

In this section, results obtained analysing the two scenarios with the proposed system are shown. The analysis is performed with both assignment algorithms; however, since the GNN algorithm produce the same result in terms of assignment, only an overall result is reported.

6.1 On-field results

The point clouds are expressed in the vessels' body frame, the results shows therefore the relative motions between the vessel and the targets.
Even if the computational time permits a higher frequency, samplings are evaluated at 1Hz in order to take into account more dense scenarios. For sake of clarity, results are plotted at a 0.25Hz frequency. Moreover, results are plotted in polar coordinates where $\underline{b_1}$ points towards 0° and $\underline{b_2}$ points towards 90° to better appreciate heading and distances.
Table 1 shows the values of the parameters used during the analysis.
In Figure 8 and Figure 9 it is reported the tracking output obtained analysing the first scenario. In particular, the identifier number of the assigned track and the point clouds are reported in Figure 8, while the obtained bounding box and the frame number are reported in Figure 9; track number 1 is reported in blue, while track number 2 is reported in orange.
The ID1 trajectory represents the relative motion between the own vessel and a moored ship. The trajectory expressed by ID2 is more complex as it is the result of the relative motion of two moving objects. Specifically, the sensor fixed to the authors' vessel travels a straight trajectory, while the pilot vessel (ID2) intersects the course from port to starboard.

In Figure 10 and Figure 11 it is reported the tracking output obtained analysing the second scenario. In particular, the identifier number of the assigned track and the point clouds are reported in Figure 10, while the obtained bounding box and the frame number are reported in Figure 11; the only track present is reported in blue.

Table 1: Values of analysis parameters

Parameter	**First scenario**	**Second scenario**
Number of frames	30	32
Time step	1 s	1 s
Cluster tracked	2	1
Cluster radius ε	7 m	5 m
minNCP	25	25
Intensity limit	15	15

 https://doi.org/10.24868/10707

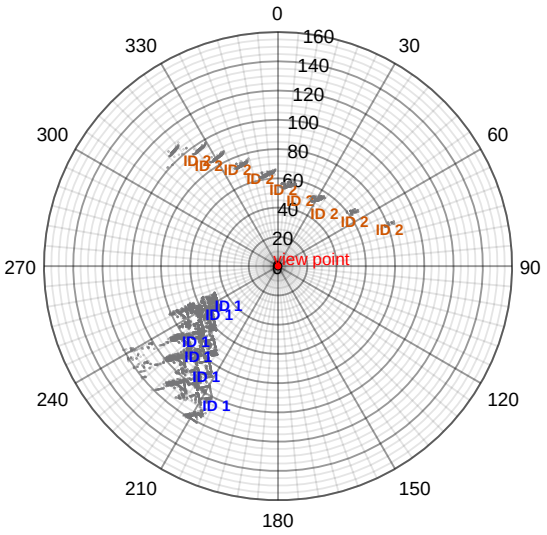

Figure 8: Point clouds and track ID, first scenario

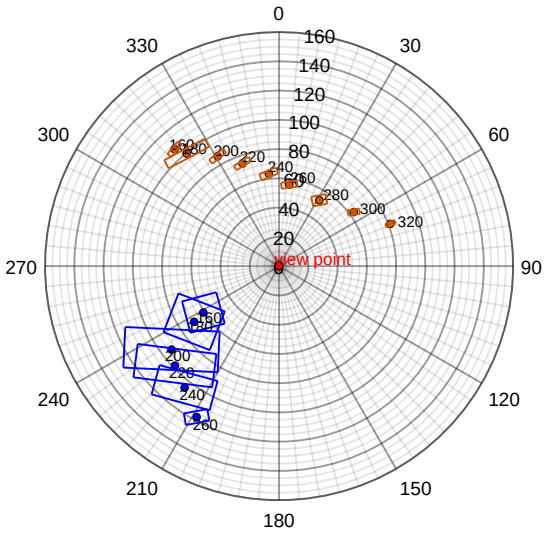

Figure 9: Obtained bounding box, first scenario

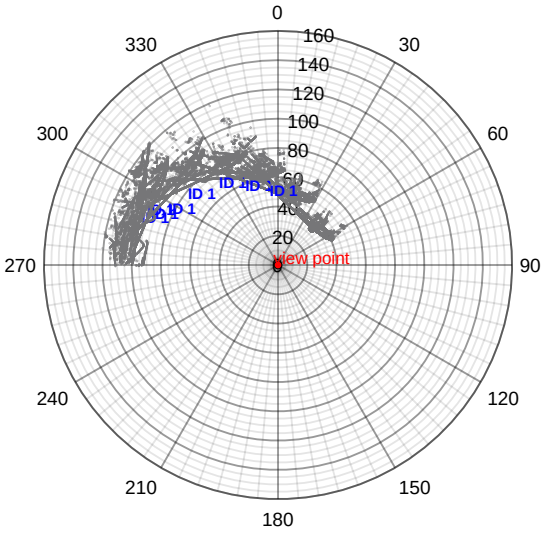

Figure 10: Point clouds and track ID, second scenario

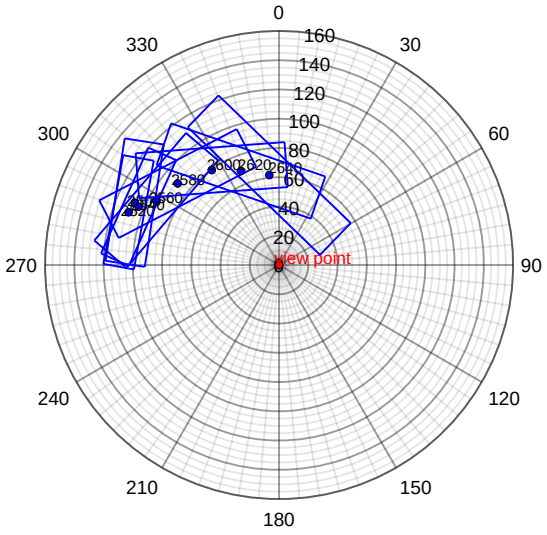

Figure 11: Obtained bounding box, second scenario

It is possible to appreciate the arcing trajectory of the target; it should be emphasised that this trajectory is completely fictitious and is due to the relative motion between the own vessel and the target. Specifically, the target is stationary at anchor and is acquired by the sensor which runs a circular path fixed to the vessel.

In Figure 12 and Figure 13 are reported the evaluated centroid's speeds for first and second scenarios respectively. The blue line with circle markers represents track number one while the orange line with cross markers represents track number 2. Since the sensor is subject to ship motions and the targets also move, the position of each other and, consequently, the point cloud acquired undergoes strong variations in some time intervals. The variation of the acquired points provides a somewhat incoherent evaluation of the centroid; this phenomenon is the main cause of the velocity fluctuations appreciable from the results shown.

6.2 Comparison

Several tracking systems and assignment algorithms are available in the literature. Of these, it was chosen to compare the proposed algorithm with GNN because both employ hard assignment, as opposed to fuzzy or soft logic employed by other algorithms. Furthermore, GNN is known and appreciated for its computational speed. The Global Nearest Neighbour is therefore an excellent yardstick for comparison.

Since the results in terms of assignment are completely overlapping, a comparison of the computational costs of the two track-assignment algorithms is reported. Figure 14 shows the computational times required to perform the entire analysis of a frame for the first and second scenario respectively. In particular, the time is divided into obstacle detection, where filtering, clustering, centroids evaluation and bounding box construction are performed,

 https://doi.org/10.24868/10707

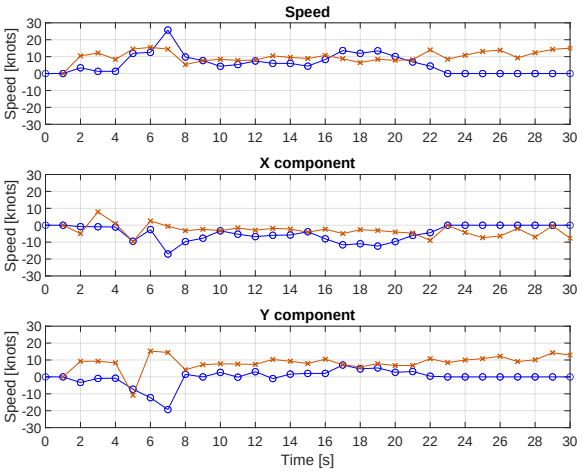

Figure 12: Cendroid speed evaluation, first scenario

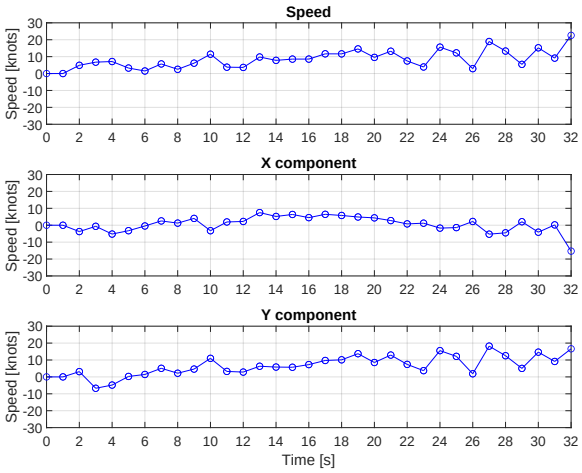

Figure 13: Cendroid speed evaluation, second scenario

and tracking, where it is performed the track association. The computational cost is referred to a standard laptop (i7-4720HQ CPU @ 2.60GHz — DDR4 16 GB). It can be noticed that the proposed assignment procedure needs a computational time of more than an order in magnitude less than the GNN, producing anyway the same result. This difference is mainly due to the lack of predictive filters.

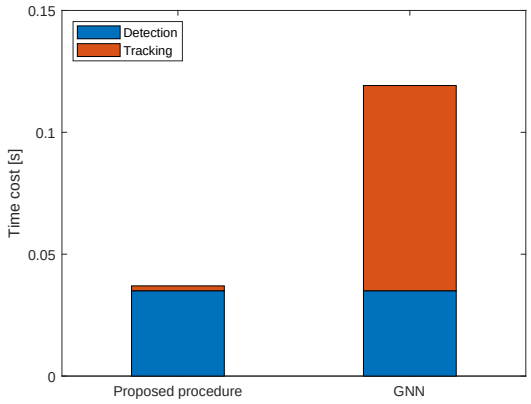

Figure 14: Time-cost comparison on a standard laptop

7 Conclusions

The proposed detection procedure based on unsupervised learning offers an alternative to the use of neural networks that require a time-consuming collection of a training dataset and the training activity itself. Such a procedure acquires a LiDAR point cloud as input and provides the bounding box and centroid of each detected obstacle. The proposed algorithm can be easily integrated with any tracking engine that requires in input a centroid, thus ensuring high flexibility of use.

Moreover, a low computational tracker is proposed and compared with the more sophisticated GNN tracker. The results obtained show how the two tracking procedures guarantee the same assignment results in the case study, while the proposed tracking system severely limits the computational resources required.

The possibility of significantly limiting the computational cost is of primary interest for detection and collision avoidance tasks in restricted spaces. Reaction time is dependent on the perception of obstacles, the proposed pro-

 https://doi.org/10.24868/10707

cedure allows targets to be identified also in case of multiple objects and short distances.
However, further steps have to be taken. Relying on a single sensor does not allow for sufficient redundancy of sources in the event of detection failure or non-acquisition. The introduction and integration of more sensors, customised for the marine environment, must be further investigated. Finally, any level of autonomy to be implemented must necessarily be assessed with current regulations, which in some cases are not yet up to date with technological developments.

8 Acknowledgements

The authors wish to thank all the staff of Cantieri Tringali Srl, particularly Dr. Marcello Tringali, for the kind availability to host us in their yard.

References

Blackman, S.; Popoli, R., 1999. Design and Analysis of Modern Tracking Systems. Artech House Radar Library.

Clunie, T., DeFilippo, M., Sacarny, M., Robinette, P., 2021. Development of a perception system for an autonomous surface vehicle using monocular camera, lidar, and marine radar, in: 2021 IEEE International Conference on Robotics and Automation (ICRA), IEEE. pp. 14112–14119.

Faggioni, N., Leonardi, N., Ponzini, F., Sebastiani, L., Martelli, M., 2022. Obstacle detection in real and synthetic harbour scenarios, in: International Conference on Modelling and Simulation for Autonomous Systems, Springer. pp. 26–38.

Fang, T.H., Han, J., Son, N.S., Kim, S.Y., 2016. Track initiation and target tracking filter using lidar for ship tracking in marine environment. Journal of Institute of Control, Robotics and Systems 22, 133–138.

Fritsch, J., Kuehnl, T., Geiger, A., 2013. A new performance measure and evaluation benchmark for road detection algorithms. 16th International IEEE Conference on Intelligent Transportation Systems (ITSC 2013) , 1693–1700.

Geiger, A., Lenz, P., Stiller, C., Urtasun, R., 2013. Vision meets robotics: The kitti dataset. International Journal of Robotics Research (IJRR) .

Han, J., Kim, J., Son, N.s., 2017. Persistent automatic tracking of multiple surface vessels by fusing radar and lidar, in: OCEANS 2017-Aberdeen, IEEE. pp. 1–5.

Iqbal, H., Campo, D., Marin-Plaza, P., Marcenaro, L., Gómez, D.M., Regazzoni, C., 2021. Modeling perception in autonomous vehicles via 3d convolutional representations on lidar. IEEE Transactions on Intelligent Transportation Systems , 1–12doi:10.1109/TITS.2021.3130974.

Jackson, J.E.A., 1988. User's Guide to Principal Components. Wiley.

Jolliffe, I.T., 2002. Principal Component Analysis. 2nd ed. Springer.

Konstantinova, P., Udvarev, A., Semerdjiev, T., 2003. A study of a target tracking algorithm using global nearest neighbor approach, in: Proceedings of the International Conference on Computer Systems and Technologies (CompSysTech'03), pp. 290–295.

Lee, K.W., Kalyan, B., Wijesoma, S., Adams, M., Hover, F.S., Patrikalakis, N.M., 2010. Tracking random finite objects using 3d-lidar in marine environments, in: Proceedings of the 2010 ACM Symposium on Applied Computing, pp. 1282–1287.

Ruud, K.A., Brekke, E.F., Eidsvik, J., 2018. Lidar extended object tracking of a maritime vessel using an ellipsoidal contour model, in: 2018 Sensor Data Fusion: Trends, Solutions, Applications (SDF), IEEE. pp. 1–6.

Schiaretti, M., Chen, L., Negenborn, R.R., 2017a. Survey on autonomous surface vessels: Part i-a new detailed definition of autonomy levels, in: International conference on computational logistics, Springer. pp. 219–233.

Schiaretti, M., Chen, L., Negenborn, R.R., 2017b. Survey on autonomous surface vessels: Part ii-categorization of 60 prototypes and future applications, in: International conference on computational logistics, Springer. pp. 234–252.

Song, X., Wang, P., Zhou, D., Zhu, R., Guan, C., Dai, Y., Yang, R., 2019. Apollocar3d: A large 3d car instance understanding benchmark for autonomous driving, pp. 5452–5462.

Zaccone, R., Martelli, M., 2020. A collision avoidance algorithm for ship guidance applications. Journal of Marine Engineering & Technology 19, 62–75.